Acta Cryst. (1964). **17**, 990

Aspherical Atomic Scattering Factors in Crystal Structure Refinement I. Coordinate and Thermal Motion Effects in a Model Centrosymmetric System

By B. Dawson

Division of Chemical Physics, C.S.I.R.O. Chemical Research Laboratories, Melbourne, Australia

(*Received* 23 *May* 1963)

The consequences of $\bar{f}$-refinement procedures on atoms whose charge distributions are intrinsically non-centrosymmetric are examined in terms of a simple hypothetical structure consisting of two sp^3 hybrid valence 'prepared' state nitrogen atoms which are centrosymmetrically disposed in a unit cell and assumed to be vibrating isotropically. The 'observed' $F(hkl)$ data based on the three f curves appropriate to the non-centrosymmetric atomic shape assumed differ considerably from the 'calculated' $\overline{F}(hkl)$ derived with the $\bar{f}$ curve which corresponds to the spherically averaged form of the atomic shape: in one instance, the R index reflecting the intrinsic shape is *ca.* 8%. The differences ΔF between F and $\overline{F}$, for data in the full Cu range and in the restricted range $0 < \sin\theta/\lambda < 0{\cdot}5$ Å^{-1}, are used to display the magnitude of shape effects $\Delta\varrho$ in Fourier line and plane sections through the atomic centre and along its symmetry axis. $\Delta\varrho$ is shown to consist of two parts, $\Delta\varrho_c$ which arises from the difference between the centrosymmetric component of the non-centrosymmetric atom and the spherically averaged treatment, and ϱ_a which represents the antisymmetric atomic component which is ignored in the spherical approximation. The features of $\Delta\varrho$ and its components are given for the thermal conditions corresponding to $\overline{B} = 1$, 2 or 3 Å^2.

The consequences of minimizing the ΔF values by the $\bar{f}$-refinement procedure are investigated briefly for 'difference' Fourier conditions and more extensively for unit-weight least-squares conditions, using both ranges of data. It is shown that the $\bar{f}$ approach introduces spurious atomic shifts (of *ca.* 0·02 Å) and considerable apparent thermal anisotropy, and that these erroneous parameter adjustments have seeming high reliability by the customary criteria of accuracy. The end result of the $\bar{f}$ treatment is the extensive elimination of the originally considerable $\Delta\varrho$ features of the atomic shape.

The results of the model examination are generalized in discussing some of the implications of acentric scattering effects in refined structure analysis. Suggestions are made regarding the types of strategy that are desirable in the future for full exploitation of precision analysis in studying the distribution of electron density around atomic centres.

Introduction

With the prospect that much of the tedium of accurate structure analysis may soon be eliminated when digital computer facilities are combined with current developments of automatic counter diffractometers, it should be possible to devote increasing attention to two general problems which require high precision for an answer. The first is that of improving the definition of structural details in a light-atom molecular system to the point where, for example, two bond lengths can be confidently stated as being significantly different to 0·01 Å: Cruickshank (1960) has pointed out the advantages that should follow the achievement of such accuracy in geometrical detail. The second is that of examining the distribution of electron density about atomic centres with a view to obtaining some experimental insight into why groups of atoms in a molecule adopt the geometries we find, and why molecules assume the form of intermolecular packing we observe. The requirements of data-accuracy of these two aims are somewhat different: the former is concerned primarily with inner-electron scattering effects which become increasingly dominant at larger values of $\sin\theta/\lambda$ — so that low temperature facilities and use of hard radiation for the data collection are desirable (Cruickshank, 1960; Dawson, 1961) — whereas the latter is concerned with outer-electron scattering effects manifesting themselves in data at smaller values of $\sin\theta/\lambda$. However, the two problems are obviously closely related since a detailed electron distribution study can only follow the successful definition of molecular geometry (and atomic thermal motion).

Apart from accuracy in experimental data, a further important condition for success in atom-centre and thermal motion precision is that the data be treated by a reduction procedure which possesses sufficient flexibility for the fine details being sought: the obvious recent example of this requirement is the development of individual anisotropic thermal motion analyses that has followed the appreciation of orientation rela-

tionships between the vibration ellipsoids of symmetry-related atoms (Rollett & Davies, 1955; Trueblood, 1956). We propose to examine this requirement by considering the role of the atomic scattering factor (f curve). Current refinement procedures are based on spherically averaged treatments of atomic scattering power (*i.e.* $\bar{f}$ curves), and the question of the adequacy of this approach was noted (Dawson, 1964*a*; hereafter I) in deriving new light-atom f curves appropriate to the aspherical charge distributions which are implied in simple $s-p$ hybrid valence state considerations. The examination reported here is concerned with the consequences of $\bar{f}$-refinement in a hypothetical structure of nitrogen atoms assumed to be in the sp^3 hybrid valence 'prepared' state approximation of I, when accurate data from such a structure are restricted in angular range by the limits associated with the commonly used Cu radiation (*i.e.* $\sin\theta/\lambda < 0{\cdot}65$ Å^{-1}). As noted in I, the charge distribution of this state of the nitrogen atom is non-centrosymmetric, and described in terms of (i) a centric component whose shape is a prolate spheroid, (ii) an antisymmetric component whose symmetry axis is coincident with that of (i). Three f curves are required to describe the scattering power of this non-centrosymmetric atom, two of which, $f_c^{\parallel}$ and $f_c^{\perp}$, relate to (i) while the third, $f_a^{\parallel}$, relates to (ii), and the acentric scattering component is $\pi/2$ out of phase with the centric components.

Features of the hypothetical structure

Consider the structure consisting of two sp^3 atoms, N(1) and N(2), disposed centrosymmetrically in a cubic unit cell (which we take to have an edge dimension of 10 Å). Orient the charge distribution of N(1) so that the positive direction of its symmetry axis (*i.e.* the positive axis of the lone pair hybrid orbital in I) is parallel to the $+\mathbf{a}$ direction of the cube, and assign the atomic centre the fractional coordinates x_1, y_1, z_1. The coordinates of N(2) are then $\bar{x}_1, \bar{y}_1, \bar{z}_1$, and the positive axis of this atom is along the $-\mathbf{a}$ direction

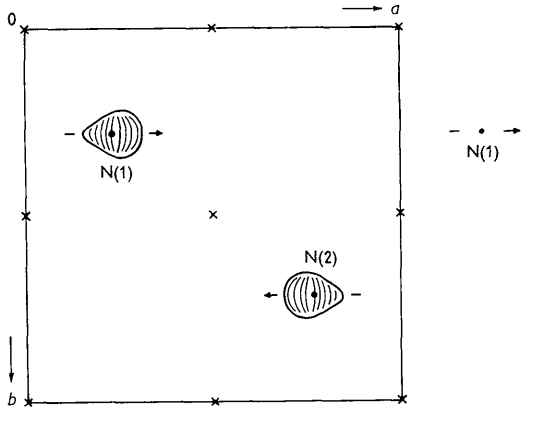

Fig. 1. The disposition of non-centrosymmetric atoms in the model structure.

(Fig. 1). Assume that the thermal motion about these positions is isotropic and described by $T_j(hkl) = \exp[-\bar{B}_j(\sin^2\theta/\lambda^2)_{hkl}]$ (j=N(1) or N(2)), so that the general structure factor expression is

$$F(hkl) = [\sum_j f_j(hkl) \exp\{2\pi i(hx_j + ky_j + lz_j)\}]T(hkl) . \quad (1)$$

For any reflexion defined by the scattering vector $\mathbf{S}$, the scattering power of the non-centrosymmetric charge distribution is, from I,

$$f(\mathbf{S}) = f_c(\mathbf{S}) + if_a(\mathbf{S}) ,$$

with

$$f_c(\mathbf{S}) = f_c^{\parallel}(S)\cos^2\Theta + f_c^{\perp}(S)\sin^2\Theta, \; f_a(\mathbf{S}) = f_a^{\parallel}(S)\cos\Theta ,$$

where $S = |\mathbf{S}| = 2\sin\theta/\lambda$ and Θ is the angle which $\mathbf{S}$ makes with the symmetry axis of the charge distribution as defined in I. The scattering powers $f_j(hkl)$ thus depend on the values of Θ_j; and for N(1), we have $\cos\Theta_1 = h/\sqrt{(h^2+k^2+l^2)}$, and for N(2), $\cos\Theta_2 = -\cos\Theta_1$. Hence, $f_c(\mathrm{N}(1)) = f_c(\mathrm{N}(2))$, but $f_a(\mathrm{N}(1)) = -f_a(\mathrm{N}(2))$, so that (1) has the form

$$F(hkl) = 2\{f_c(hkl)\cos\varphi_1 - f_a(hkl)\sin\varphi_1\}T(hkl) , \quad (2)$$

where $\varphi_1 = (hx_1 + ky_1 + lz_1)$, and the values of $f_c(hkl)$ and $f_a(hkl)$ are governed by the three f curves in I and the values $\Theta_1(hkl)$.

If we ignore the non-centrosymmetric shape of the charge distribution, and describe the atomic scattering power in the customary spherically averaged form, $\bar{f}_c = \frac{1}{3}(f_c^{\parallel} + 2f_c^{\perp})$, then, since $\bar{f}_a = 0(1)$ now becomes

$$\bar{F}(hkl) = 2\bar{f}_c(hkl)\cos\varphi_1 . T(hkl) . \quad (3)$$

The differences between (2) and (3) reflect the influence of the intrinsic shape of the non-centrosymmetric atom, and a difference Fourier synthesis composed of terms $(F-\bar{F})$ over a range of possible (hkl) data will display the magnitude of shape features, $\Delta\varrho$, ignored by the $\bar{f}$ approach. From (2), we see that $\Delta\varrho = \Delta\varrho_c + \varrho_a$, where $\Delta\varrho_c$ displays the deviations of the centric aspherical charge distribution component from the spherically averaged approximation, and ϱ_a is the antisymmetric component which is absent in the spherical treatment. The two components can be evaluated separately by assigning N(1) the coordinates $(\frac{1}{4}, \frac{1}{4}, \frac{1}{4})$ in (2) and (3), since then $\sin\varphi_1 = 0$ for $(h+k+l) = 2n$ and $\cos\varphi_1 = 0$ for $(h+k+l) = 2n+1$.

When values of $\bar{B} = 1$ or 2 Å^2 are used to obtain F- and $\bar{F}$-data over the complete range of reflexions accessible to Cu radiation (*i.e.* $0 < \sin\theta/\lambda < 0{\cdot}65$ Å^{-1}), the magnitudes of $\Delta\varrho$, $\Delta\varrho_c$ and ϱ_a along the symmetry axis of N(1) (*i.e.* along the line $x, \frac{1}{4}, \frac{1}{4}$) are as shown in Fig. 2(*a*). Fig. 2(*b*) compares the three-dimensional (3-D) result in Fig. 2(*a*) for $\bar{B} = 2$ Å^2 with the corresponding 2-D result given by $(hk0)$ data. This comparison is extended in Fig. 2(*c*) to illustrate the features of $\Delta\varrho_c$ and ϱ_a in the plane of the atomic centre and the symmetry axis. The features along the symmetry axis of the acentric atom are further summarized in Table 1.

Table 1. *Characteristics of non-centrosymmetric sp^3 N(1) for different data ranges and different thermal motions*

	$0<\sin\theta/\lambda<0{\cdot}65$ Å^{-1}				$0<\sin\theta/\lambda\leq 0{\cdot}50$ Å^{-1}			
	$\bar{B}=1$ Å^2	$\bar{B}=2$ Å^2	$\bar{B}=3$ Å^2		$\bar{B}=1$ Å^2	$\bar{B}=2$ Å^2	$\bar{B}=3$ Å^2	
	3-D	3-D	3-D	(2-D)	3-D	(2-D)	3-D	(2-D)	3-D	(2-D)
$\Delta\varrho_c$(max)	+0·43 e.Å^{-3}	+0·34	+0·28	(+0·21)	+0·27	(+0·25)	+0·23	(+0·21)	+0·20	(+0·19)
at $\Delta x=$	±0·55 Å	±0·55	±0·56	(±0·62)	±0·67	(±0·69)	±0·68	(±0·70)	±0·69	(±0·71)
$\Delta\varrho_c$(min)										
at $\Delta x=0$	0·0	0·0	0·0	(−0·18)	0·0	(−0·18)	0·0	(−0·16)	0·0	(−0·14)
	(−0·25 e.Å^{-3})	(−0·21)								
ϱ_a(max)	+0·60 e.Å^{-3}	+0·50	+0·43	(+0·43)	+0·46	(+0·50)	+0·41	(+0·45)	+0·36	(+0·40)
at $\Delta x=$	+0·38 Å	+0·39	+0·39	(+0·39)	+0·46	(+0·44)	+0·46	(+0·45)	+0·47	(+0·46)
$\Delta\varrho$(max)	+0·99 e.Å^{-3}	+0·81	+0·68	(+0·60)	+0·70	(+0·67)	+0·61	(+0·60)	+0·53	(+0·53)
at $\Delta x=$	+0·45 Å	+0·46	+0·47	(+0·50)	+0·54	(+0·55)	+0·54	(+0·55)	+0·54	(+0·56)
	(+0·80 e.Å^{-2})	(+0·68)								
	(+0·48 Å)	(+0·49)								
$\Delta\varrho$(min)	−0·33 e.Å^{-3}	−0·28	−0·24	(−0·39)	−0·28	(−0·45)	−0·25	(−0·41)	−0·23	(−0·36)
at $\Delta x=$	−0·25 Å	−0·26	−0·27	(−0·23)	−0·33	(−0·28)	−0·34	(−0·29)	−0·35	(−0·29)
	(−0·51 e.Å^{-2})	(−0·45)								
	(−0·21 Å)	(−0·22)								
$\partial\Delta\varrho/\partial x$	+2·51 e.Å^{-4}	+2·05	+1·70	(+2·01)	+1·61	(+1·80)	+1·40	(+1·60)	+1·22	(+1·42)
at $\Delta x=0$	(+2·36 e.Å^{-3})									
$\bar{\varrho}$(max)	— e.Å^{-3}	13·4	11·2	(8·9)	—	(9·1)	9·1	(8·3)	8·1	(7·6)
at $\Delta x=0$	(11·6 e.Å^{-2})	(10·1)								
$\partial^2\bar{\varrho}/\partial w^2$	— e.Å^{-5}	−133·4	103·2	(−85·8)	—	(−70·1)	−58·0	(−60·4)	−49·5	(−52·3)
at $\Delta x=0$	(−135·7 e.Å^{-4})	(−107·2)								
∂x-shift	— Å	+0·015	+0·017	(+0·020)	—	(+0·026)	+0·024	(+0·027)	+0·025	(+0·027)
	(+0·017 Å)	(+0·019)								

The values of the maxima (and minima) of $\Delta\varrho$ and its components, the distances, Δx, from the atomic centre at which these values occur, the slopes of $\Delta\varrho$ at the atomic centre (*i.e.* the values of $\partial\varrho_a/\partial x$ at $x=x_1$), and the values of the spherically averaged peak height,

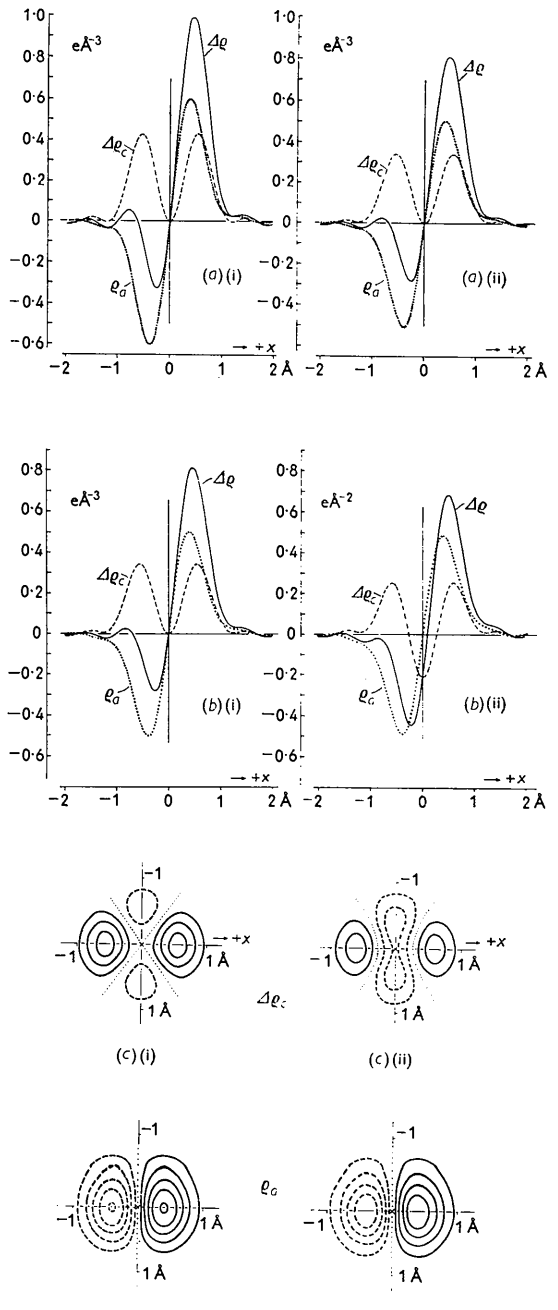

Fig. 2. Fourier sections for N(1) along the line, x, ¼, ¼ or in the plane $x, y,$ ¼ of Fig. 1 to illustrate the shape features $\Delta\varrho$ and its two components $\Delta\varrho_c$ and ϱ_a: (*a*) (i) and (*a*) (ii) are for $F(hkl)$ data with $\bar{B}=1$ and 2Å^2 respectively; (*b*) (i) is (*a*) (ii) and (*b*) (ii) is the corresponding result for $F(hk0)$ data; (*c*) (i) and (*c*) (ii) are expanded versions of $\Delta\varrho_c$ and ϱ_a in (*b*), with contours drawn at intervals of 0·1 e.Å^{-2}.

$\bar{\varrho}$, and curvature, $\partial^2\bar{\varrho}/\partial x^2$, of N(1) at its centre, using (3), are given for 3-D and 2-D sets of data corresponding to the three $\bar{B}$ values, 1, 2 and 3 Å^2. The results for the full Cu range of data are compared with those for the restricted range $0 < \sin\theta/\lambda \leq 0{\cdot}50$ Å^{-1}.

The two components associated with the approximation of spherical averaging are seen to build up on one side of the atom to a considerable composite peak, whose height is roughly that of a hydrogen atom. The size of these residual features is naturally dependent on the degree of thermal motion, but the dependence is not very marked since outer-electron scattering is involved: of almost equal importance to thermal motion is the angular range of data used in examining these features. The results for sets of 2-D and 3-D data are numerically quite similar, the major difference being that $\Delta\varrho_c$ is not zero at the atomic centre in the 2-D situation. This is understandable, however, from the nature of the atomic 'shapes' in the two cases. In the 3-D case, the prolate spheroidal shape with scattering powers of $f_c^{\parallel}, f_c^{\perp}, f_c^{\perp}$ along the three principal axes of the spheroid is matched exactly by the spherically averaged treatment using $\bar{f}_c = (f_c^{\parallel}+f_c^{\perp}+f_c^{\perp})/3$, and, consequently, $\Delta\varrho_c$ is zero at the atomic centre. In the 2-D case considered, the projected elliptical shape with scattering powers of $f_c^{\parallel}, f_c^{\perp}$ along the two principal axes is not matched by the $\bar{f}_c$-treatment, and $\Delta\varrho_c$ is no longer zero at the atomic centre since it reflects the negative values $(f_c^{\parallel}-f_c^{\perp})/6$ by which the elliptically and spherically averaged scattering powers differ.*

Refinement of the structure

If we ignore the origin of these residual features, and consider only their overall appearance and distribution about the atomic centre, then it is apparent that an $\bar{f}$ approach will interpret them as evidence of imprecise definition of atomic position and thermal motion (and possibly of scale factor adjustment in the 2-D situation). In the 'difference' Fourier method (Cochran, 1951), the features of ϱ_a will result in N(1) being shifted from its true position by the amounts δx given in Table 1. The shifts there vary from 0·015 to 0·027 Å, and are seen to be governed more by the angular range of the diffraction data employed than by the atom's intrinsic thermal motion.

The same general conclusions apply to least-squares $\bar{f}$-refinement. We shall examine this approach further since it provides a convenient method of investigating the simultaneous adjustment (and interaction) of position and thermal parameter modifications, and we shall minimize the residual $r = \Sigma w(F-\bar{F})^2$ summed over a range of (hkl) data. For simplicity, we will take unit weights throughout and confine the minimization of r to $(hk0)$ data containing $\bar{B}=2$ Å^2, but we shall generalize the earlier situation by moving N(1) from its special position to $x_1=0{\cdot}20$, $y_1=0{\cdot}30$ so that there are now both f_c and f_a contributions to all $F(hk0)$. The adjustable parameters to be considered, for both of the sin θ/λ ranges noted previously, are x, B_{11} and B_{22}, and a scale factor k to allow for possible change in the 'observed' $F(hk0)$ arising from the finite value of $\Delta\varrho_c$ at the atomic centre.

The progress of two cycles of adjustment in each data range is summarized in Table 2. We see there that the initial R indices $(R=100\Sigma(F-\bar{F})/\Sigma\bar{F})$ of *ca.* 8%, which are based on $\bar{F}(hk0)$ values derived from the correct position and thermal motion but the wrong $(\bar{f})$ scattering description, are significantly reduced when the $\bar{f}$ treatment is allowed to introduce a spurious atomic shift and anisotropic vibration into the calculation of 'better' values of $\bar{F}(hk0)$. The effect of these adjustments is also reflected in the dramatic reduction in the values of r. Since this residual is involved in the estimation of the standard deviations (s.d.) of the parameters being varied, the values of r thus give very small estimates for the results ultimately reached (Table 2). There is no indication that the final parameters deviate from the correct ones by amounts which are extremely large by the normal criteria based on these standard deviations.

The normalized inverse matrices (see *e.g.* Geller, 1961) in Table 2 show that there is very little correlation between the coordinate adjustment and the other variable parameters. This is to be expected from the simpler picture in Fig. 2 and Table 1 obtained with N(1) at the special position, and we may therefore use the convenient diagonal least-squares approximation to estimate the shifts $\delta x'$ of the atom in our general position when $\bar{B}$ has the values 1 and 3 Å^2. For the extended (and restricted) ranges, the shifts thus obtained are, in Å, 0·024 (0·031) for $\bar{B}=1$ and 0·027 (0·034) for $\bar{B}=3$ Å^2. By comparison, the first cycle shifts for $\bar{B}=2$ Å^2 — using either the full matrix procedure actually employed or the diagonal simplification — are 0·027 (0·033), and it is seen that the trend in $\delta x'$ with angular range and $\bar{B}$ factor follows that of the Fourier estimates δx in Table 1.

The numerical differences between δx and $\delta x'$ arise from the influence of the weighting scheme on the spurious adjustments. The Fourier approach is effectively a minimization of r when $w=1/\bar{f}$, where $\bar{f}$ is the temperature-modified scattering power of each reflexion (Cochran, 1948, 1951; Cruickshank, 1952), so that the influence of the various $(F-\bar{F})$ terms in the minimization of r increases with sin θ/λ. The diminution in importance of the non-spherical scattering effects with increasing sin θ/λ thus results in the Fourier process indicating smaller parameter adjustments than those given by the unit-weight least-squares treatment. The differences between the two

* This applies only to the orientation chosen for N(1) in the model structure, and to the use of $F(hk0)$ data (as here) or $F(h0l)$ data. For $F(0kl)$ data, N(1) is circular in projection, with scattering power $f_c^{\perp}$, and the use of the $\bar{f}$ treatment would result in a positive value of $\Delta\varrho_c$ at the centre, which would reflect the positive values $(f_c^{\perp}-f_c^{\parallel})/3$ by which the two f approaches now differ.

Table 2. *Unit-weight least-squares $\bar{f}$-refinement of non-centrosymmetric* N(1)

	$0<\sin\theta/\lambda<0{\cdot}65$ Å^{-1}				$0<\sin\theta/\lambda\leq 0{\cdot}50$ Å^{-1}			
Cycle	0	1	2	$\sigma(2)$	0	1*	2	$\sigma(2)$
x (Å)	2·000	2·027	2·029	(0·001)	2·000	2·027	2·034	(0·001)
B_{11} (Å^2)	2·00	2·54	2·57	(0·043)	2·00	2·54	2·76	(0·048)
B_{22} (Å^2)	2·00	1·66	1·68	(0·038)	2·00	1·66	1·57	(0·044)
k†	1·000	1·006	1·002	(0·003)	1·000	1·006	1·002	(0·003)
R (%)	8·1	3·8	3·8		8·3	2·7	2·3	
r	5·240	0·964	0·940		4·967	0·622	0·376	

Correlation matrices from first cycle

	$0<\sin\theta/\lambda<0{\cdot}65$ Å^{-1}				$0<\sin\theta/\lambda\leq 0{\cdot}50$ Å^{-1}			
	x	B_{11}	B_{22}	k	x	B_{11}	B_{22}	k
x	1	−0·0058	−0·0008	−0·0024	1	−0·0094	−0·0014	−0·0037
B_{11}		1	−0·0655	0·4492		1	0·0053	0·5044
B_{22}			1	0·4584			1	0·5121
k				1				1

* The results listed here differ from those of the first least-squares cycle over this range but apply to the values of R and r shown in this column. The actual results obtained were $x=2{\cdot}033$ Å, $B_{11}=2{\cdot}77$ Å^2, $B_{22}=1{\cdot}55$ Å^2, but values of R and r based on these results were not computed.

† The scale factor is that to be applied to the initial $F(hk0)$.

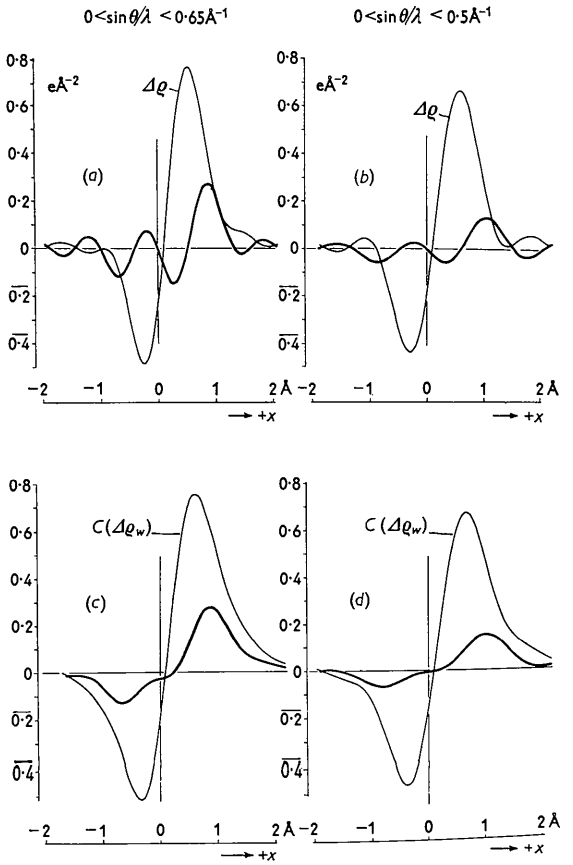

Fig. 3. Line sections (related to (*b*) (ii) of Fig. 2) illustrating the differences between conditions for difference Fourier and unit-weight least-squares refinement: (*a*) and (*b*) are normal Fourier sections, over the extended and limited sin θ/λ ranges respectively, showing the cancellation of the original $\Delta\varrho$ features (lighter lines) by the least-squares parameter adjustments which produce the heavier lines; (*c*) and (*d*) are corresponding weighted Fourier plots which simulate the least-squares conditions (see text).

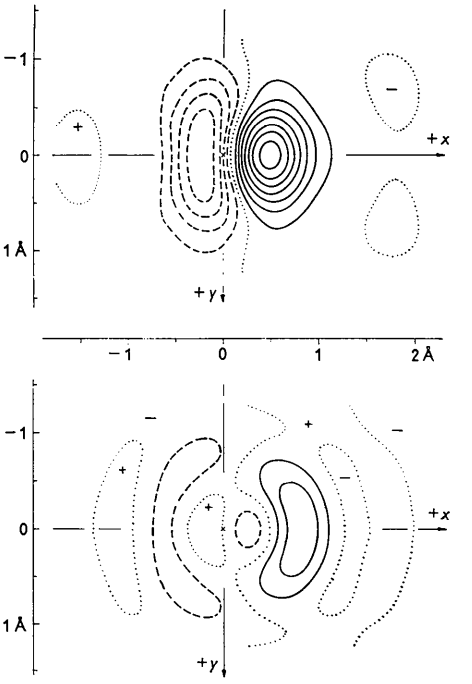

Fig. 4. An extended illustration of Fig. 3(*a*): the upper half of the diagram shows the true $\Delta\varrho$, and the lower half the residue after the least-squares parameter adjustment. Contours are at 0·1 e.Å^{-2} intervals, positive as full lines, negative as broken lines, and zero as dotted lines.

sets of adjustments are illustrated in the line sections along the symmetry axis of N(1) shown in Fig. 3. Fig. 3(*a*) and (*b*) are for the extended and restricted ranges respectively, and show the modifications of the normal Fourier shape features of $\Delta\varrho$ when the second-cycle unit-weight least-squares parameters are used to obtain $\bar{F}(hk0)$ data. The resultant difference sections (shown as the heavier lines in the figure) have an appreciable reversed slope at the atom position,

indicating that the $\delta x'$ values are an over-correction for the Fourier conditions. The least-squares conditions are simulated in difference Fourier form in Fig. 3(*c*) and (*d*), where line sections corresponding to (*a*) and (*b*), but derived from weighted syntheses containing terms $C\bar{f}(F-\bar{F})$, show that the initial slope at the atomic centre has been eliminated by the $\delta x'$ adjustment: C is a constant chosen so that the peak height of $\Delta\varrho_w$ in the initial weighted syntheses is the same as that in the normal syntheses in Fig. 3(*a*) and (*b*).

Apart from these technical differences in δx and $\delta x'$ (and also B_{11} *etc.*), the main feature of Fig. 3 is its demonstration of the efficiency with which the acentric scattering effects of N have been absorbed into an $\bar{f}$ approach by the introduction of spurious parameter adjustments. Fig. 4 displays the sections of Fig. 3(*a*)* in more-extensive two-dimensional from, and it is seen that most of the significant and recognizable information associated with the shape of the charge distribution has been eliminated in the $\bar{f}$ procedure.

Discussion

It is clear that the results of the examination here have a bearing on both of the general aims of precision structure analysis noted in the Introduction, and it is therefore desirable to consider their implications in a context which is broader than the assumptions made in our model study of the adequacy of current methods of structure refinement based on the $\bar{f}$ approach. Basically, we have, (i) taken a specific light-atom type, N, (ii) assigned it a specific charge distribution non-centrosymmetry based on the $s-p$ hybrid orbital considerations developed in I, (iii) assumed a centrosymmetric disposition of such atoms in a unit cell (we shall not discuss the case of non-centrosymmetric disposition here), and, (iv) imposed on the relevant $F(hkl)$ data the upper limit of angular range associated with Cu radiation: and we have found that neglect of the atomic shape by an $\bar{f}$-refinement causes, firstly, the production of spurious atomic shifts and thermal vibration parameters which are seemingly highly reliable by R and r factor and s.d. criteria, and, secondly, the consequent elimination of quite marked information regarding the shape deviations from spherical symmetry. The possibility that extensive refinement involving anisotropic temperature factor adjustment may absorb aspherical scattering effects has been occasionally noted in the past but the influence of charge distribution acentricity on atom-centre location in atoms heavier than hydrogen has not been recognized.

For the conditions (iii) and (iv) above, the results obtained for N may be regarded as representative of those which apply to other second-row atoms in 'prepared' states involving acentric charge distributions of the type assumed in (ii). In the heavier O and F, the greater slope of ϱ_a arising from the greater angular extension of f_a'' with $\sin\theta/\lambda$ (see Table 1 and Fig. 4 of I) will offset the greater peak curvature of these atoms; while in the atoms lighter than C, the smaller peak curvature should be matched by a diminution in the slope of ϱ_a arising from the more diffuse nature of the antisymmetric charge distribution component which accompanies the reduction in nuclear charge. The present study thus suggests that, in situations where the conditions (ii) — (iv) are approached, the application of $\bar{f}$-refinement procedures can lead to the misplacement of second-row atoms by *ca.* 0·02 Å and to the introduction of quite large temperature factor errors. In the case of the related third-row atoms, the analogous spurious adjustments will obviously be much smaller: the spherically symmetric inner-electron scattering dominating the central curvatures will be much greater, and the slopes of ϱ_a will be much reduced because of the smaller angular range of f_a^{II} (*cf.* the second- and third-row analogues in Fig. 4 of I). However, here again, the spurious shifts obtained with accurate data will be greater than errors covered by the normal criteria of parameter reliability noted above.

Clearly, the crux of the matter in any practical situation where we wish to make a precision study (which henceforth we shall assume to concern only second-row atoms) lies in the angular range of the accurate diffraction data collected for the examination. Aspherical or acentric scattering effects will naturally vary in magnitude with environment (see I), and their unprejudiced detection in a detailed electron distribution study so as to examine their possible influence as a structure-determining factor may well be the ultimate aim of an investigation (see below). The results obtained here show that the essential prerequisite of precision in the structural parameters is unlikely to be satisfied if instrumental limitations or other factors restrict the range of data collection to that available with Cu radiation. The desirability of an accurate experimental technique incorporating Mo or Ag radiation and low temperature facilities which extend data-measurement to higher values of $\sin\theta/\lambda$, and thus permit the valid use of $\bar{f}$ curves in parameter refinement (Dawson, 1961), is consequently made more pressing.

The magnitude of the experimental problem of accurate measurement over such an extended range becomes extremely formidable, however, and many cases will arise where precise data cannot be obtained beyond $\sin\theta/\lambda \simeq 0{\cdot}6$ Å^{-1} for structures in which there may be reasonable expectation that acentric scattering is present. In these circumstances, two lines of attack on the problem of shape effects appear feasible. The first is to subject the data to two forms of refinement procedure, initially using the current $\bar{f}$ approach and

* It may be observed that the peak height of $\Delta\varrho$ of N(1) in the general position here differs slightly from that in Fig. 2(*b*) for the earlier special position. This difference arises from the fact the 'general' $F(hk0)$ sample the f curves at half the interval of the 'special' $F(hk0)$, and the f curves do not vary linearly between the coarser sampling points.

subsequently using an approach which incorporates f curves of the type developed in I. The positional and thermal parameters ultimately derived from the two approaches will differ; and the validity of the f curves used in the latter approach, for any particular system being studied, will be indicated by the further reduction in R and r factors which is possible because of the incomplete allowance for shape effects made by the $\bar{f}$ curve treatment and its spurious parameter adjustments (see the second-cycle R and r residuals in Table 2). The availability of digital computers makes the implementation of this dual approach by the least-squares method most attractive, since it would permit rapid testing of different possibilities in the non-$\bar{f}$ approach. It will be necessary, however, to employ programs which permit evaluation of the different $f(hkl)$ contributions which may apply to various members of a symmetry-related set of atoms (Dawson, 1964*b*) when the convenient $\bar{f}$-treatment used hitherto is abandoned, and such programs have not been developed. Careful thought will also have to be given to the difficult problem of what constitutes the most satisfactory weighting scheme (and what constitute reliable tests of its suitability) in any particular set of data (Cruickshank, Pilling, Bujosa, Lovell & Truter, 1961), and the usefulness of this line of attack on shape effects requires development on several fronts. The second line of attack lies in a combination of precise neutron and X-ray $\bar{f}$-refinements. Provided the standard deviations of the sets of structural parameters defined by the two techniques are small enough, then significant differences between the sets could be assessed in terms of X-ray shape features of the type considered here and in I. Alternatively, if it is valid to assume that the neutron diffraction values of atomic position and, particularly, thermal motion (Calder, Cochran, Griffiths & Lowde, 1962) are applicable to the X-ray data, then a 'difference' procedure with $\bar{f}$ curves and these parameters should reveal the magnitude and disposition of shape effects that may be present.

One can only speculate on these matters at the present stage, but the important point is recognition of the possibility that significant information on molecular structure — other than that of detailed stereochemistry — may be forthcoming when highly accurate X-ray data can be obtained by the development of suitable automatic diffractometers. The directional properties of lone pairs in hybrid orbitals, and their influence either in hydrogen bond formation (Schneider, 1955) or in donor molecules which may form more-general donor-acceptor complexes (Hassel & Rømming, 1962), represents a broad field in which useful tests of this theoretical concept should be possible in future detailed investigations. Further discussion of systems which appear suitable for intensive study of possible charge distribution accntricity will be given later (Dawson, 1964*c*).

References

Calder, R. S., Cochran, W., Griffiths, D. & Lowde, R. D. (1962). *J. Phys. Chem. Solids*, **23**, 621.

Cochran, W. (1948). *Acta Cryst.* **1**, 138.

Cochran, W. (1951). *Acta Cryst.* **4**, 408.

Cruickshank, D. W. J. (1952). *Acta Cryst.* **5**, 511.

Cruickshank, D. W. J. (1960). *Acta Cryst.* **13**, 774.

Cruickshank, D. W. J., Pilling, D. E. & (in part) Bujosa, A., Lovell, F. M. & Truter, M. R. (1961). *Computing Methods and the Phase Problem in X-ray Crystal Analysis*. Oxford: Pergamon Press.

Dawson, B. (1961). *Acta Cryst.* **14**, 1271.

Dawson, B. (1964*a*). *Acta Cryst.* **17**, 997.

Dawson, B. (1964*b*). To be published.

Dawson, B. (1964*c*). To be published.

Geller, S. (1961). *Acta Cryst.* **14**, 1026.

Hassel, O. & Rømming, C. (1962). *Quart. Rev. Chem. Soc., Lond.* **16**, 1.

Rollett, J. S. & Davies, D. R. (1955). *Acta Cryst.* **8**, 125.

Schneider, W. G. (1955). *J. Chem. Phys.* **23**, 26.

Trueblood, K. N. (1956). *Acta Cryst.* **9**, 359.